

Supporting information

Ultra-Stable Binder-Free Rechargeable Li/I₂ Battery Enabled by “Betadine” Chemical Interaction

Zhen Meng^{ad}, Xiaojian Tan^a, Shunlong Zhang^a, Hangjun Ying^{ad}, Xufeng Yan^{ad}, Huajun Tian^{*b},
Guoxiu Wang^b, Wei-Qiang Han^{*,a,c}

^a Ningbo Institute of Material Technology and Engineering, Chinese Academy of Sciences, Ningbo 315201, P. R. China.

^b Centre for Clean Energy Technology, University of Technology Sydney, Broadway, Sydney, NSW 2007, Australia.

^c School of Materials Science and Engineering, Zhejiang University, Hangzhou 310027, P. R. China.

^d University of Chinese Academy of Sciences, Beijing 100049, P.R. China

*Email: hanwq@zju.edu.cn or Huajun.Tian@uts.edu.au

Content

1. Experimental Sections.....	3
2. Characterization of the ACC and PVP-I ₂	4
3. The electrochemical performances of the ACC/PVP-I ₂ cathodes, ACC and some Li/iodine batteries.	8
4. References	13

1. Experimental Sections

Preparation of ACC/PVP-I₂ cathodes. To prepare the cathodes with iodine loading of 1.6-1.8 mg cm⁻², the ethanol solution method was used. Namely, 1.2 g of PVP-I₂ was first dissolved in 8 ml of ethanol to obtain the PVP-I₂/ethanol solution. Then the ACC was immersed in this solution. After 8 hours, the ACC was taken out. The extra PVP-I₂/ethanol solution on the ACC surface was soaked up by tissue. Then the ACC/PVP-I₂ cathode was dried under vacuum for several minutes. The cathodes with iodine loading of 2.5 mg cm⁻² and 3.1 mg cm⁻² was prepared in the same procedure except that the ACC was immersed in the PVP-I₂/ethanol solution for 12 hours and 24 hours, respectively.

Electrochemical tests. CR2032 coin cells were assembled in an Ar-filled glove box with Li-metal anode and ACC/PVP-I₂ cathode. The diameter of one ACC/PVP-I₂ cathode electrode is 0.8 cm. The area iodine loading for the ACC/PVP-I₂ cathode determined by the ion chromatography was 1.6-1.8 mg cm⁻², 2.5 mg cm⁻² and 3.1 mg cm⁻². The weigh percentage of the iodine in the electrode was 10.2-10.6 wt% for the cathodes with iodine loading of 1.6-1.8 mg cm⁻². The electrolyte was 1M LiN(CF₃SO₂)₂ (LiTFSI) in a 1:1 v/v mixture of 1,3-dioxolane/1,2-dimethoxyethane (DOL/DME) containing 1 wt% of LiNO₃. Galvanostatic discharge/charge tests were performed by cycling between 2.0 - 3.6 V.

Material characterization. Scanning electron microscope (SEM) measurements and energy dispersive X-ray spectroscopy (EDS) were taken using FEI Quanta FEG 250 field emission microscopy. Thermogravimetric analysis (TGA) was performed by a Pyris Diamond analyzer under nitrogen flow with a heating rate of 5 °C min⁻¹. Raman spectra were obtained with a Renishaw inVia Reflex Raman spectrometer. Laser excitation at 532 nm was employed to get the Raman spectra of I₂⁵ and I₂³. For the Raman spectra of C=O in the PVP, laser excitation at 633 nm was used. Ion chromatography was obtained by DIONEX ICS-1100 ion chromatograph.

Density functional calculations. The first-principles calculations were performed by using a pseudopotential method as implemented in the vasp code.¹ The exchange correlation energy was in the form of Perdew-Burke-Ernzerhof with generalized gradient approximation.² The plain-wave cutoff was set as 500 eV, and 10 × 1 × 1 Monkhorst-Pack *k*-mesh was generated for the systems. A vacuum region of 20 Å was set to separate the ACC/PVP-I₂ chains, and the structures were determined until the magnitude of the force became less than 0.02 eV/Å. To modify the exchange and correlation energies of hydrogen bonding, the van der Waals-augmented density functional theory of functional optB88-vdW was adopted.³ Then we used the nudged elastic band (NEB)⁴ method to investigate the activation barriers for the adsorption of I₂ on the systems.

2. Characterization of the ACC and PVP-I₂

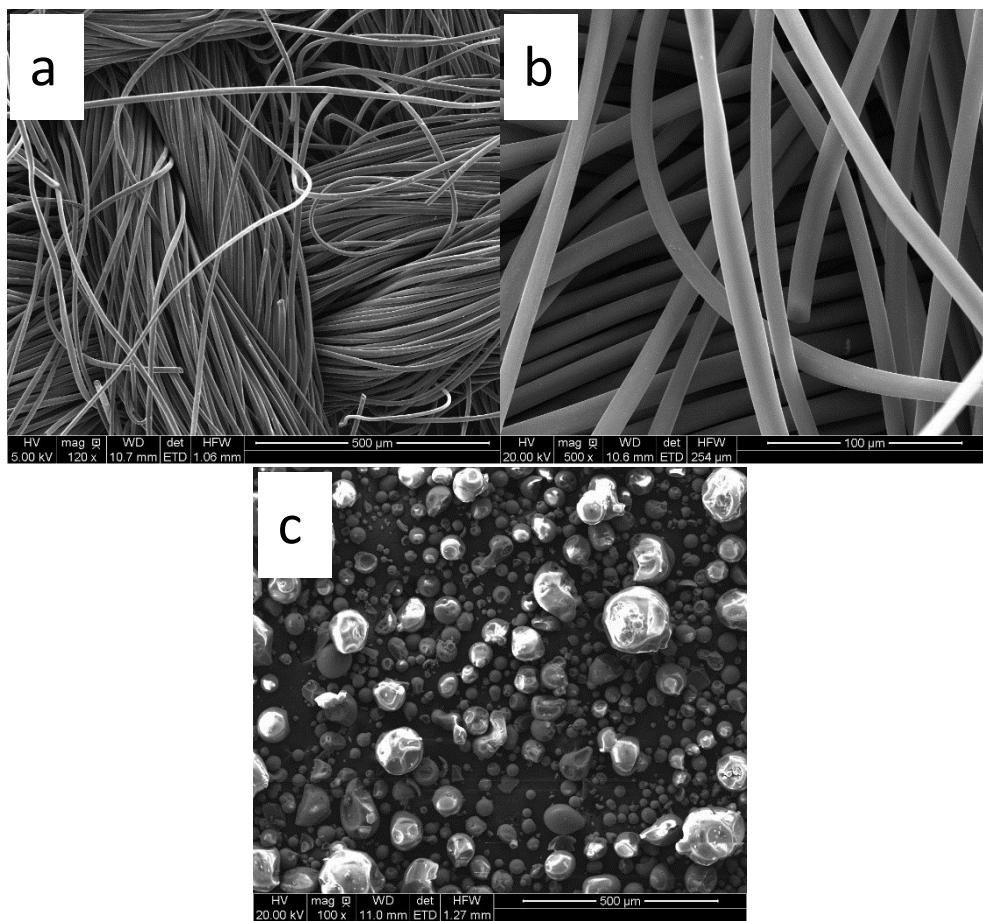


Figure S1. SEM images of the ACC (a and b) and PVP-I₂ (c).

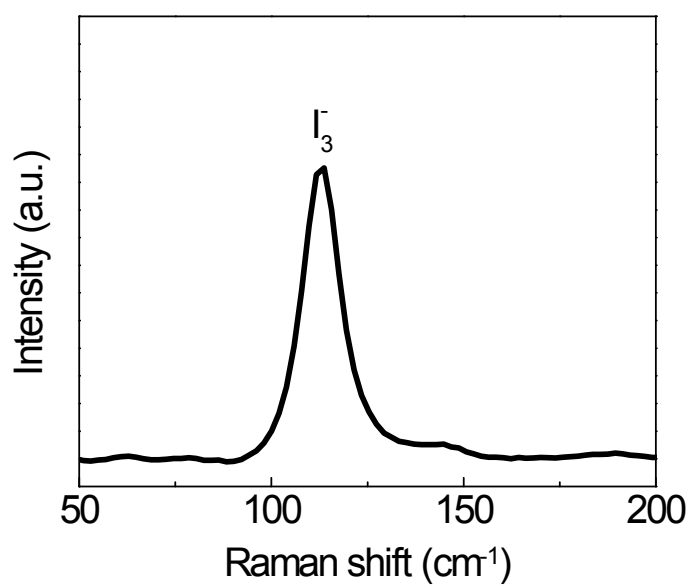


Figure S2. Raman spectrum of the PVP-I₂.

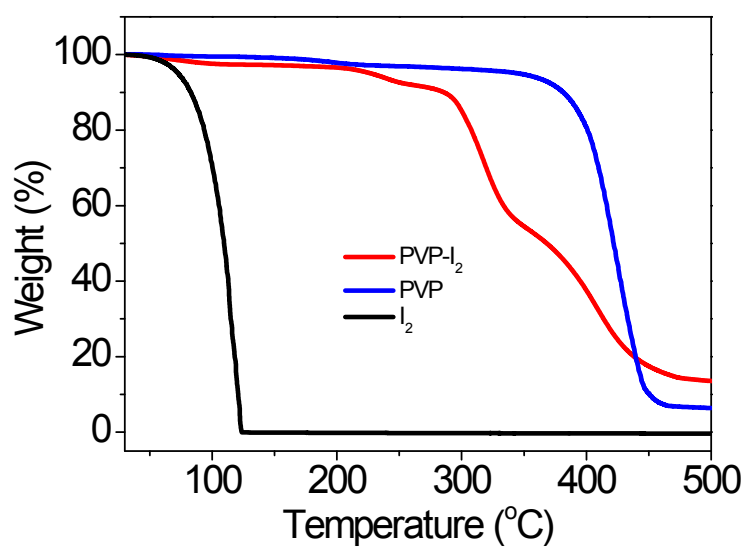


Figure S3. TGA curves of the I₂, PVP and PVP-I₂.

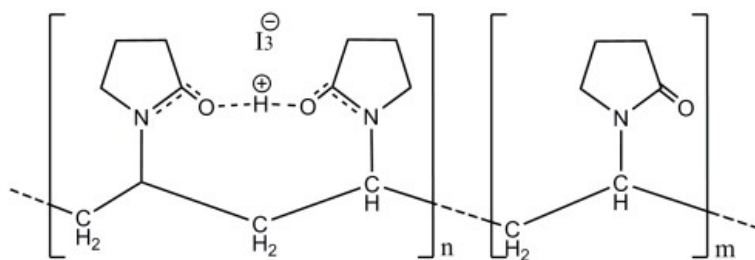


Figure S4. Proposed structure of the PVP-I₂.⁵

According to the articles reported, there are two kinds of interaction between PVP and iodine. One is the hydrogen bond.^{5, 6} As shown in Figure 2.2a, HI₃ bound to the PVP framework via the hydrogen bond between the proton and the carbonyl group. The other is the charge transfer interaction.^{7, 8} In this interaction, iodine act as electron acceptor and nitrogen atom act as electron donor.^{8, 9} This two kinds of interaction coexist in the PVP-I₂ cathode, which could trap most of the iodine species in the PVP framework.

3. The electrochemical performances of the ACC/PVP-I₂ cathodes, ACC and some Li/iodine batteries.

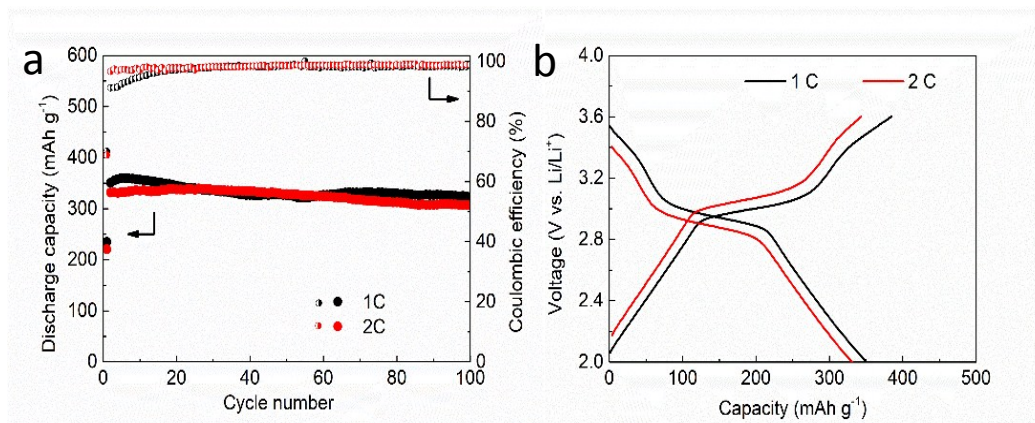


Figure S5. Electrochemical performance of the batteries with ACC/PVP-I₂ cathodes at 1C and 2C: (a) cycle performance; (b) voltage profiles.

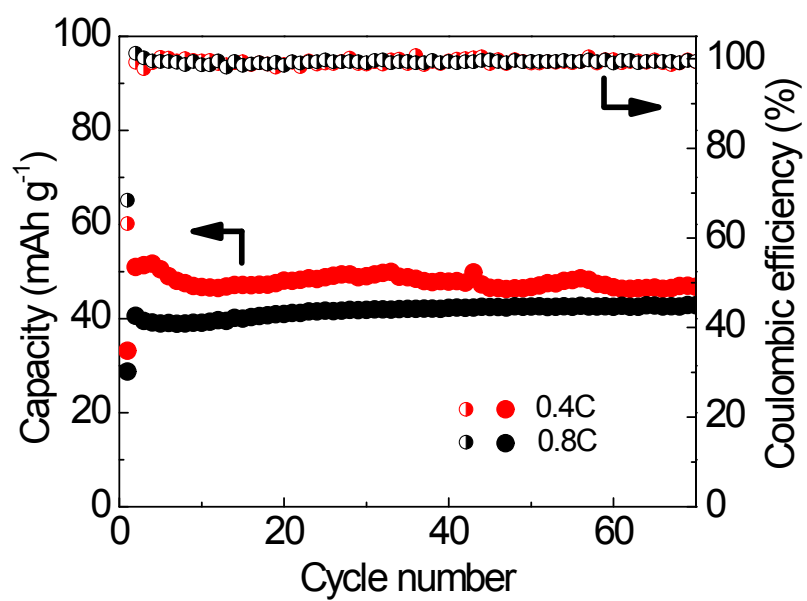


Figure S6. The electrochemical performances of the ACC. For the 0.4C and 0.8C cells, the charge/discharge currents are the same as the ACC/PVP-I₂ cathode cycled at 0.4C and 0.8 C, respectively.

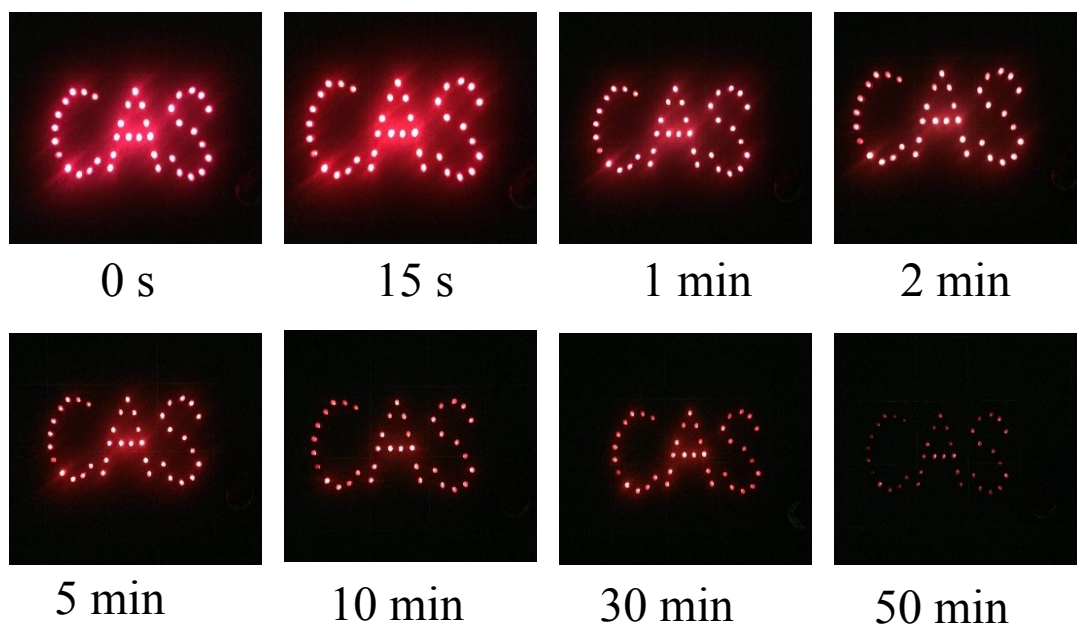


Figure S7. The brightness of the LEDs powered by a coin cell depending on time.

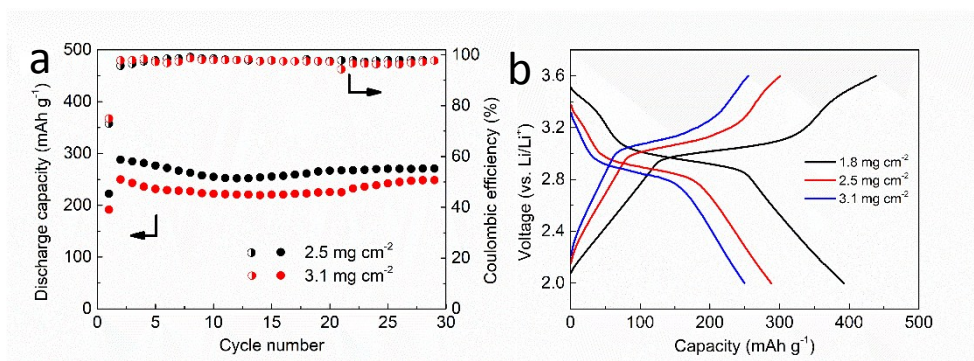


Figure S8. (a) Cycle performance of the cathodes with higher iodine loading at 0.4C. (b) Voltage profiles in the 2nd cycle of the cathodes with various iodine loadings at 0.4C.

The electrochemical performance of the cells with higher iodine loading at 0.4C was also measured (Figure S8a). The discharge capacities of the cells with iodine loading of 2.5 and 3.1 mg cm⁻² at the 2nd cycle were 288 and 249.8 mAh g⁻¹, respectively. After 30 cycles, they still exhibited discharge capacities of 270.9 and 248.5 mAh g⁻¹, respectively. In addition, higher polarization could be observed in the battery with higher iodine loading (Figure S8b).

Table S1. The comparison of the cycle performance between our ACC/PVP-I₂ cathode and other Li/iodine batteries reported.

Cathode material	C-rate (current density)	Cycle number/Discharge capacity	Capacity retention/Capacity decay rate	Ref.
Iodine/N-FHS	5C	200/~190 mA h g ⁻¹	84%/-	10
B ₂ O ₃ /carbon microtube composite interlayer	20C	500/176.9 mA h g ⁻¹	88%/0.023%	11
Iodine/Nanoporous Carbon	0.5C	300/195 mA h g ⁻¹	65%/0.12%	12
I ₂ -HPCM-NP	500 mA g ⁻¹	2000/~250 mA h g ⁻¹	84.5%/-	13
ACC/PVP-I ₂	8C	2400/240 mA h g ⁻¹	81%/0.0079% (2nd to the 2400th cycle)	This work

4. References

1. G. Kresse and J. Furthmüller, *Phys. Rev. B*, 1996, **54**, 11169-11186.
2. J. P. Perdew, K. Burke and M. Ernzerhof, *Phys. Rev. Lett.*, 1996, **77**, 3865-3868.
3. S. Savasta, O. D. Stefano, V. Savona and W. Langbein, *Phys. Rev. Lett.*, 2005, **94**, 246401.
4. G. Henkelman, B. P. Uberuaga and H. Jónsson, *J. Chem. Phys.*, 2000, **113**, 9901-9904.
5. H.-U. Schenck, P. Simak and E. Haedicke, *J. Pharm. Sci.*, 1979, **68**, 1505-1509.
6. S. Moulay, *J. Poly. Eng.*, 2013, **33**, 389-443.
7. K. Takikawa, M. Nakano and T. Arita, *Chem. Pharm. Bull.*, 1978, **26**, 1370-1374.
8. J. Wu, P. Li, S. Hao, H. Yang and Z. Lan, *Electrochim. Acta*, 2007, **52**, 5334-5338.
9. Z. Küçükyavuz, S. Küçükyavuz and N. Abbasnejad, *Polymer*, 1996, **37**, 3215-3218.
10. K. Li, B. Lin, Q. Li, H. Wang, S. Zhang and C. Deng, *ACS Appl. Mater. Inter*, 2017, **9**, 20508-20518.
11. Z. Su, C.-J. Tong, D.-Q. He, C. Lai, L.-M. Liu, C. Wang and K. Xi, *J. Mater. Chem. A*, 2016, **4**, 8541-8547.
12. Q. Zhao, Y. Lu, Z. Zhu, Z. Tao and J. Chen, *Nano Lett.*, 2015, **15**, 5982-5987.
13. K. Lu, Z. Hu, J. Ma, H. Ma, L. Dai and J. Zhang, *Nat. Commun.*, 2017, **8**, 527.